Transcriptome analyses reveal the toxicity of graphene oxide with different diameters on buckwheat root growth

Changying Liu^{1,2}*, Hanlin Wang^{1,2}, Han Li³, Qingcheng Qiu^{1,2}, Dabing Xiang^{1,2}, Yanxia Liu³*

¹Key Laboratory of Coarse Cereal Processing, Ministry of Agriculture and Rural Affairs, Sichuan Engineering and Technology Research Center of Coarse Cereal Industralization, Chengdu University, Chengdu, Sichuan, PR China

Citation: Liu C.Y., Wang H.L., Li H., Qiu Q.C., Xiang D.B., Liu Y.X. (2024): Transcriptome analyses reveal the toxicity of graphene oxide with different diameters on buckwheat root growth. Czech J. Genet. Plant Breed., 60: 237–248.

Abstract: Graphene-based materials (GBMs) have become potential soil pollutants due to their wide applications in agricultural environments. Although physiological mechanisms of plant responses to GBMs have been previously explored, the underlying molecular mechanisms remain unclear. In this paper, we analysed the physiological and transcriptomic changes of buckwheat (*Fagopyrum* spp.) roots exposed to 100 mg/L graphene oxide (GO) with different diameter. GO negatively affected root growth and higher diameters of GO caused more adverse effects on the root. In total 3 724 GO-responsive genes were identified in root by transcriptome analysis. 70 differentially expressed genes (DEGs) were involved in ROS detoxification, and 37 transporter-encoding genes were found to be involved in GO response. These transporters may regulate the uptake and transport of GO in buckwheat. The gene expression of 84 transcription factors (TFs) showed a response to GO stress in the root, which may regulate the transporters and reactive oxygen species (ROS) detoxification-related genes. Finally, the difference in the transcriptomic response of the root to the three GO materials with different diameters was investigated. 49 GO-responsive genes may be involved in the difference in the toxicity of GO with different diameters. This study provides new insights into the molecular mechanisms of plant roots to GBMs.

Keywords: buckwheat; graphene oxide; phytotoxicity; transcriptome analysis

Graphene is a two-dimensional carbon-based nanomaterial composed of monolayer carbon atoms (Zhao et al. 2022a). Graphene and graphene-based materials (GBMs) have been widely used in various fields, including electronics, optical industries, biosensors, semiconductors, pipes, solid-phase ex-

traction, packaging, medicine and agriculture (Hu et al. 2018; Alamdari et al. 2019). As far, there are many kinds of GBMs produced from graphene, such as graphene quantum dots, graphene oxide (GO) and reduced GO (rGO) (Zhang et al. 2022). Of these GBMs, GO have better characteristics than other

Supported by National Natural Sciences Foundation of China (No. 32301850), the Science and Technology Project of Guizhou Branch of China Tobacco Corporation (2023XM08), the Science and Technology Project of China Tobacco Corporation (110202202015), China Agriculture Research System (No. CARS-07-B-1), and Sichuan Science and Technology Program (No. 2023NSFSC0214).

²School of Food and Biological Engineering, Chengdu University, Chengdu, Sichuan, PR China

³Guizhou Academy of Tobacco Science, Guiyang, Guizhou, PR China

^{*}Corresponding author: lcyswu@163.com; liuyanxia306@163.com

[©] The authors. This work is licensed under a Creative Commons Attribution-NonCommercial 4.0 International (CC BY-NC 4.0).

GBMs, with excellent physiological stability, biocompatibility and hydrophilicity (Yang et al. 2022). GO is the oxidized form of graphene that contains extensive oxidative modifications in its basal plane (Poulsen et al. 2021). Nowadays, GO was extensively produced and widely applied in many areas, which will gradually be released into the environment, and ultimately affecting ecosystems and organisms (Sun et al. 2019; Zhao et al. 2023). Previous studies suggested that GBMs can enter into human (Homo sapiens), mice and zebrafish (Danio rerio), and brains, lung, liver, umbilical vein endothelial cells and neural stem cells were damaged by GBMs (Sun et al. 2019; Tang et al. 2019; Luo et al. 2021; Poulsen et al. 2021). Therefore, the underlying environmental behaviour and ecological toxicity of GO on organisms should be deeply elucidated.

Plants often suffer from numerous contaminated stress conditions, and some pollutants can be absorbed by plants and then enter into the food chain (Liu et al. 2022). Previous studies in Arabidopsis, buckwheat (Fagopyrum spp.), lettuce (Lactuca sativa L.) and wheat (Triticum aestivum L.) suggested that GO can enter into plant cell and result in toxic effects on plant growth (Zhao et al. 2015; Gao et al. 2020; Weng et al. 2020; Liu et al. 2022). GO with high concentrations significantly inhibited seed germination, rhizome elongation, plant growth and biomass (Cheng et al. 2016; Weng et al. 2020; Zhang et al. 2020; Lee et al. 2021). How GO adversely affect the growth of plants? A previous study showed that 50~100 mg/L GO treatment inhibited root growth of Brassica napus L. by affecting abscisic acid (ABA) and indole-3-acetic acid (IAA) biosynthesis (Cheng et al. 2016). Recent studies in alfalfa and white clover (Trifolium repens L.) suggested that GO can suppress plant growth and root development by inducing structural impairment, photosynthesis inhibition, oxidative stress, and nutrient imbalance (Zhao et al. 2022b, 2023). Although the ecotoxicological risk of GO on plant was studied in above studies, more studies are needed to investigate the detailed physiological mechanisms.

The molecular mechanisms of plant responses to GO have been preliminary explored. In tomato (Solanum lycopersicum L.), GO inhibited the expression of IAA-responsive gene and induced root development-related genes (Guo et al. 2021). In apple (Malus domestica), GO modulated adventitious root growth by regulating the expression of auxin efflux carrier, auxin influx carrier and cytokinin

(CTK) biosynthetic enzyme encoding genes (Li et al. 2018). In *B. napus*, GO regulates root growth via regulating many hormone pathway signaling genes' expression (Xie et al. 2019, 2020). Additionally, GO exposure suppressed wheat root activity and NO_3^- uptake by inhibiting nitrate transporter encoding gene' expression (Weng et al. 2020). However, the molecular mechanism of plant response to GO needs to be deeply investigated.

Previous studies suggested the differences in the size of nanomaterials resulted in distinct toxicity in plants. For example, single-walled carbon nanotubes exhibit the strongest phytotoxic effect as compared to multi-walled carbon nanotubes (Basiuk et al. 2019). For GBMs, 200 mg/L of graphene with 1-2 layers promoted wheat root elongation, while graphene with < 30 layers inhibited rice root growth (Liu et al. 2015; Zhang et al. 2016). In Aloe vera L., 0-100 mg/L GO with few layers could increase the morphological characters and yield of root and leaf and enhance the photosynthetic capacity of leaves (Zhang et al. 2021b). In buckwheat, 100 mg/L GO with < 3 layers and the diameter of 0.5-3 µm significantly inhibited buckwheat root growth (Liu et al. 2022). In wheat, single-layer GO treatment induced a more severe inhibitory effect on root growth than multi-layer GO (Zhu et al. 2022). It is suggested that the layer numbers have significant impact on the toxicity of GO on plants. However, there is no report on the phytotoxicity of GO with different sizes at other dimensions, such as diameter.

Buckwheat is a pseudocereal crop belonging to Polygonaceae family and Fagopyrum genus, which was considered as a good model plant to investigate the regulatory mechanisms of crops respond to hazardous materials (Liu et al. 2022; Zhang et al. 2023). In our previous study, it was found that high concentrations of GO inhibited buckwheat seedlings growth, and GO can penetrate into buckwheat root and stem cells (Liu et al. 2022). In addition, buckwheat roots exhibited significant physiological and transcriptomic responses to GO (Liu et al. 2022). However, the detailed molecular mechanisms of buckwheat root respond to GO are needed to be explored. In this study, the GO materials with different diameters were used to treat buckwheat seedlings, and the physiological and transcriptomic response of root were analysed. This paper will improve our knowledge on the molecular responsive mechanism of plant root to the toxicity of GO.

MATERIAL AND METHODS

Plant material and growth conditions. A widely cultivated buckwheat variety, Chuanqiao No. 1, was used. The buckwheat seeds were sterilized by 0.1% KMnO₄ and washed by ddH₂O, and then placed in culture plates for germination (Liu et al. 2022). The three-day-old seedlings were placed in the culture plates containing 100 mg/L GO with three different diameters, which were purchased from the Chengdu Organic Chemicals Co. Ltd., Chinese Academy of Sciences (Chengdu, China). The GO with diameters of 0.5-3, 8-15 and $> 50 \mu m$ were selected for this study, which were named as GO-0, GO-10 and GO-50, respectively. The layers, thickness and ash content of the three GO materials are < 3, 0.55-1.2 nm and < 1.5 %, respectively. Finally, the roots of 10-day-old seedlings that were cultivated in a growth chamber (light 24/dark 20 °C, 14/10 h) were collected.

Morphology and biochemical analysis of seed-lings. The seedlings which were treated with 0 and 100 mg/L GO were collected. The roots of seedlings were scanned using a scanner (Epson 12000XL, Beijing, China). The length and weight of the root were recorded, respectively.

As described in our previous study, the contents of hydrogen peroxide (H_2O_2) and malondialdehyde (MDA), and the activities of peroxidase (POD) and catalase (CAT) were measured using their respective test kits (Liu et al. 2022).

Transcriptome profiling analysis. The roots that were treated with 0 and 100 mg/L GO (GO-0, GO-10 and GO-50) were collected for transcriptomic sequencing. Each experiment had three biological replicates. The methods of RNA extraction, RNA libraries construction and Illumina sequencing were performed as described in our previous studies (Liu et al. 2021, 2022). The raw data of transcriptome sequencing was submitted to NCBI Short Read Archive database (accession number: PRJNA1020781). The raw data were filtered and then mapped to the buckwheat genome (http:// mbkbase.org/Pinku1/) by using HISAT2 (Ver. 2.2.1) software. The gene expression level was estimated by reads per kilobases per million reads (RPKM). The differentially expressed genes (DEGs) between the two different samples were identified in the DEseq2 package (Ver. 1.10.1), and *P*-value < 0.05 and |log2FC| > 1 was set as the cut-off. Gene ontology enrichment of the DEGs was analysed by GOseq R package.

The correlation of the expression patterns between different DEGs was analysed by Pearson's correla-

tion coefficient, and the correlation index > 0.95 or < -0.95 was set as the threshold for correlation analysis. Finally, Cytoscape (Ver. 2.8.2) software was used to display the result of correlation analysis (Shannon et al. 2003).

Quantitative real-time PCR (qRT-PCR) analysis. The seedling roots, which were treated with 0 and 100 mg/L GO, were collected for qRT-PCR analysis. All the experimental procedures for qRT-PCR, including RNA extraction, cDNA synthesis and qRT-PCR reaction, were performed as described in a previous study (Liu et al. 2021). The reactive system for qRT-PCR analysis was prepared using SYBR® Green Realtime PCR Master Mix kit (TOYOBO, Osaka, Japan). The qRT-PCR reactions were conducted by using qTOWER3 G Real-Time PCR System (Analytik Jena AG, Germany), and all the reactions were performed in three biological replicates. FtACTIN7 gene was used as an internal control and gene' expression was performed using $2^{-\Delta\Delta Ct}$ method. Twelve genes were selected for qRT-PCR validation, and their primers used in this study are specified in Table S1 in Electronic Supplementary Material (ESM).

Statistical analysis. The data of morphology, biochemical and qRT-PCR analysis were processed by Microsoft Excel 2019 (Microsoft, Redmond, WA, USA), the significant differences were analysed by SPSS 25.0 software (SPSS Inc., Chicago, IL, USA) with Duncan multiple-range test, and the graphics were displayed by GraphPad prism 9 (GraphPad Software, La Jolla, USA).

RESULTS

The effect of GO on buckwheat root by morphology and biochemical analyses. Our previous study demonstrated that 100 mg/L is the critical concentration of GO for influencing buckwheat growth (Liu et al. 2022), and thus 100 mg/L GO with different diameters were used to treat buckwheat in this study. The weight and length of root under GO stress were evaluated. The length and weight of root were significantly suppressed by GO treatments (Figure 1). The effect of GO-10 and GO-50 on root growth is stronger than that of GO-0 (Figure 1, Figure S1 in ESM), which indicates that higher diameters of GO may cause more adverse effects on the root.

The roots that were treated with or without GO were collected for biochemical analysis. The contents of MDA and H₂O₂, as well as CAT activity in the root, were significantly improved under GO treat-

ment (Figure 1C–E). POD activity was significantly inhibited by GO (Figure 1F). These results are similar to the data that were reported in our previous study (Liu et al. 2022). Additionally, GO with greater diameters exhibited greater effects on MDA content and the activities of CAT and POD (Figure 1), which suggested that the effect of GO on root growth may depend on its size. However, the H₂O₂ contents of roots have no significant difference among the three GO materials treatments, which may be affected by other factors.

Identification of DEGs in root under GO stress by transcriptome analysis. Transcriptome profiling of buckwheat root under GO stress was performed, and more than 494 million clean reads were obtained (Table S2 in ESM). The clean data was matched to the buckwheat genome, and most sequences of CK (91.19~91.35%), GO-0 (90.65~92.05%), GO-10 (91.4~92.87%) and GO-50 (91.8~91.97%) were matched (Table S2 in ESM).

The DEGs in the root under GO stress were identified. 2 255 DEGs, including 877 up- and 1 378 down-regulated genes, were found between CK and GO-0 (CK vs GO-0). 3 155 DEGs, including 1 231 up- and

1 924 down-regulated genes, were found between CK and GO-10 (CK vs GO-10). 1 114 DEGs including 643 up- and 501 down-regulated genes were found between CK and GO-50 (CK vs GO-50) (Figure 2A). It is interesting that the number of DEGs in CK vs GO-50 is lower than another two comparisons. The accuracy of transcriptome data was confirmed by qRT-PCR analysis. As shown in Figure S2 in ESM, the expression patterns of the 12 selected genes calculated by qRT-PCR exhibited good accordance with transcriptomic expression data.

Expression and gene ontology enrichment analysis of GO-responsive DEGs. The DEGs between CK and GO were compared by Venn diagram analysis, and 3 724 GO-responsive DEGs were generated (Figure 2B). All these DEGs are mainly showing two different expression patterns (Figure 2C). Gene ontology enrichment analysis showed these DEGs were more enriched into membrane (GO: 0016020), integral component of membrane (GO: 0016021), oxidation-reduction process (GO: 0055114), protein phosphorylation (GO: 0006468), regulation of transcription DNA-templated (GO: 0006355), transmembrane transport (GO: 0055085), ATP bind-

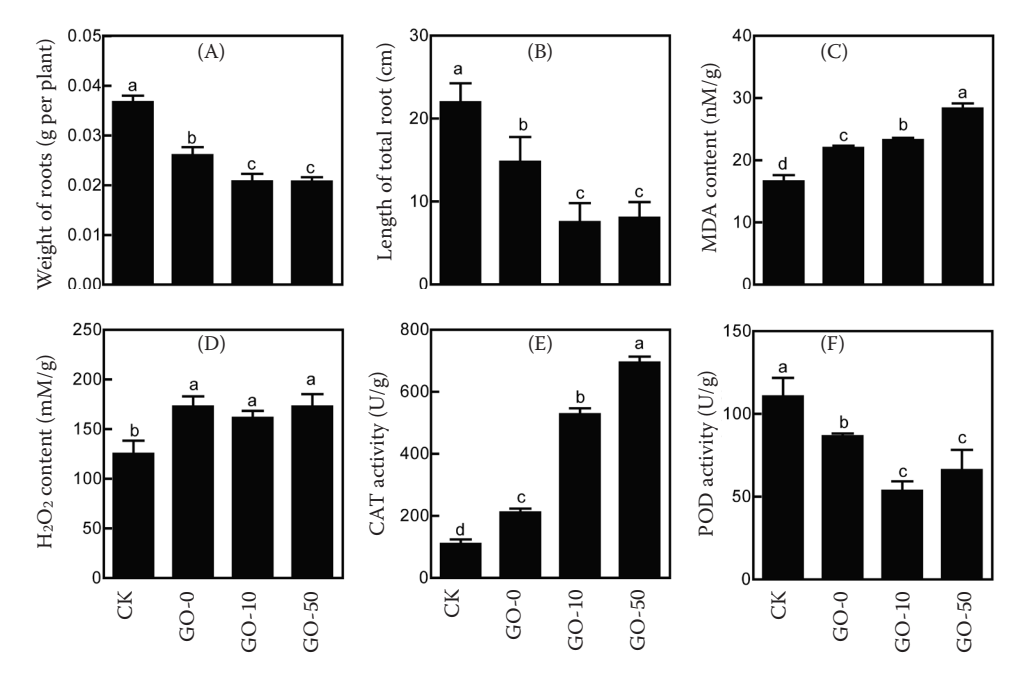


Figure 1. The effect of graphene oxide (GO) on buckwheat root growth: root weight under GO treatment (A), root length under GO treatment (B), the malondial dehyde (MDA) content of root under GO treatment (C), the hydrogen peroxide (H_2O_2) content of root under GO treatment (D), catalase (CAT) activity of root under GO treatment (E), peroxidase (POD) activity of root under GO treatment (F)

The means were compared by Duncan's test; data are means \pm SDs; significant differences (P < 0.05) are marked with different letters; CK represents the root treated with 0 mg/L GO; GO-0, GO-10 and GO-50 represent the GO with diameters of 0.5–3, 8–15 and >50 μ m, respectively

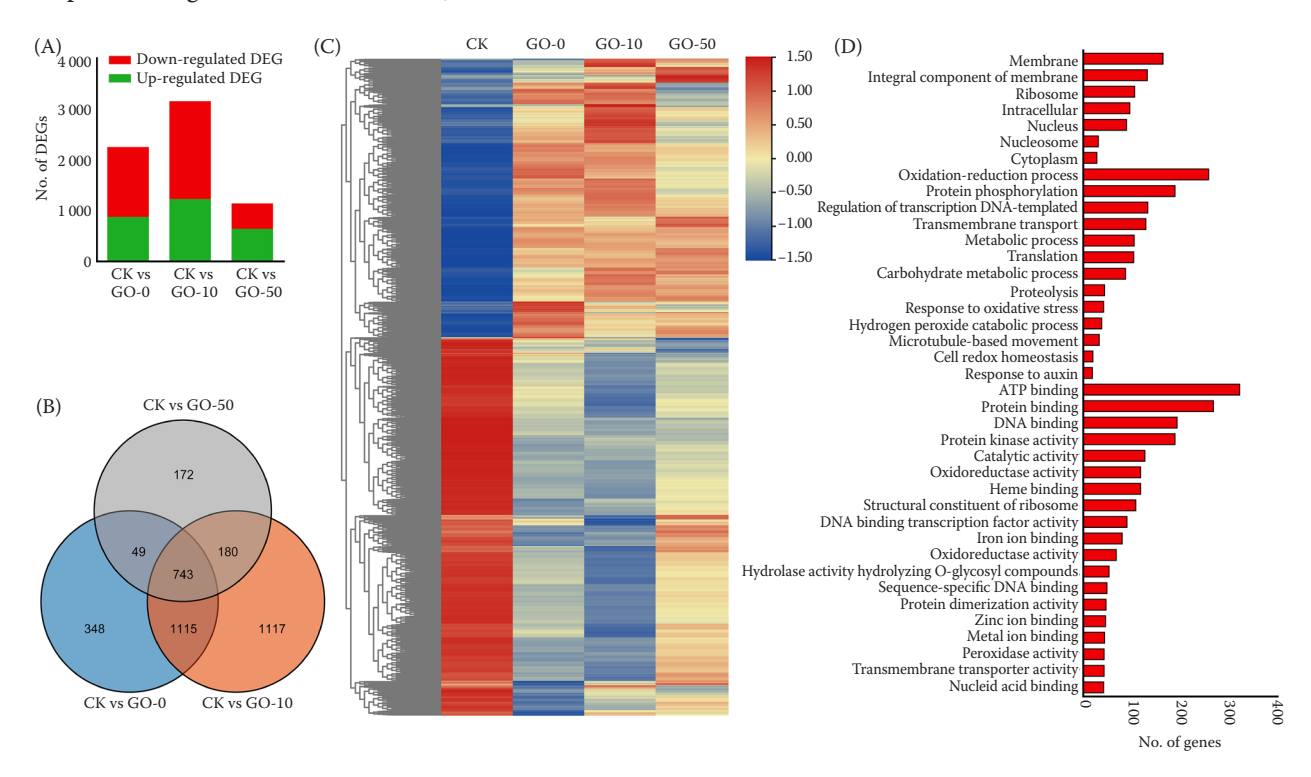


Figure 2. Identification of graphene oxide (GO)-responsive genes in root: the number of differentially expressed genes (DEGs) among the three comparisons (A), Venn diagram showing the overlapping DEGs among the three comparisons (B), heatmap of the DEGs (C), gene ontology enrichment analysis (D)

Colour scale indicates the degree of expression; red – high expression; blue – low expression; CK represents the root treated with 0 mg/L GO; GO-0, GO-10 and GO-50 represent the GO with diameters of 0.5–3, 8–15 and > 50 μ m, respectively

ing (GO: 0005524), protein binding (GO: 0005515), DNA binding (GO: 0003677) and protein kinase activity (GO: 0004672) (Figure 2D).

Identification of DEGs involved in reactive oxy**gen species (ROS) detoxification.** The above results of biochemical analysis showed GO may affect the root growth by regulating ROS detoxification, and thus the genes participating in ROS detoxification were analysed. In total 70 DEGs involved in ROS detoxification were identified, including 42 peroxidase (PER), 17 glutathione S-transferase (GST), seven glutaredoxin (GRX) and four L-ascorbate oxidase (ASO) (Table S3 in ESM). Within the 42 *FtPER* genes, 13 FtPER genes' expression was down-regulated by all the GO treatments, while the expression levels of 15 FtPER genes were up-regulated by GO (Figure 3A). The expression of 14 FtPER genes was downregulated by GO-0 and GO-10 treatments, but these genes showed no response to GO-50. Of the seven FtGRX genes, the expression of FtGRX4/6/10 was down-regulated by GO, while the other four FtGRX genes' expression was up-regulated (Figure 3B). Most of *GST* genes' expression was significantly enhanced by GO stress, and expression of all the *ASO* genes was inhibited (Figure 3C–D). In addition, five putative ROS detoxification-related genes, including four late embryogenesis abundant protein (LEA) and one respiratory burst oxidase (RBOH) encoding genes, were found (Table S3 in ESM). The expression of *FtLEA5/34* was up-regulated by GO, while *FtLEA14-A/65* and *FtRBOHH* expression was downregulated (Figure 3E, Table S3 in ESM).

Identification of DEGs encoding transporters. Our previous study preliminarily identified some transporters may be involved in the uptake and transport of GO in buckwheat (Liu et al. 2022). In this study, 37 DEGs encoding transporters were also identified, including 26 ATP-binding cassette (ABC) transporters, three sulfate transporters (SULTRs), three zinc transporters (ZIPs), two magnesium transporters (MRS), one copper transporter (COPT), one Fe transport protein (IRT) and one silicon efflux transporter (LSI) encoding genes (Table S4 in ESM). Of the 26 FtABC genes, 13 genes' expression was

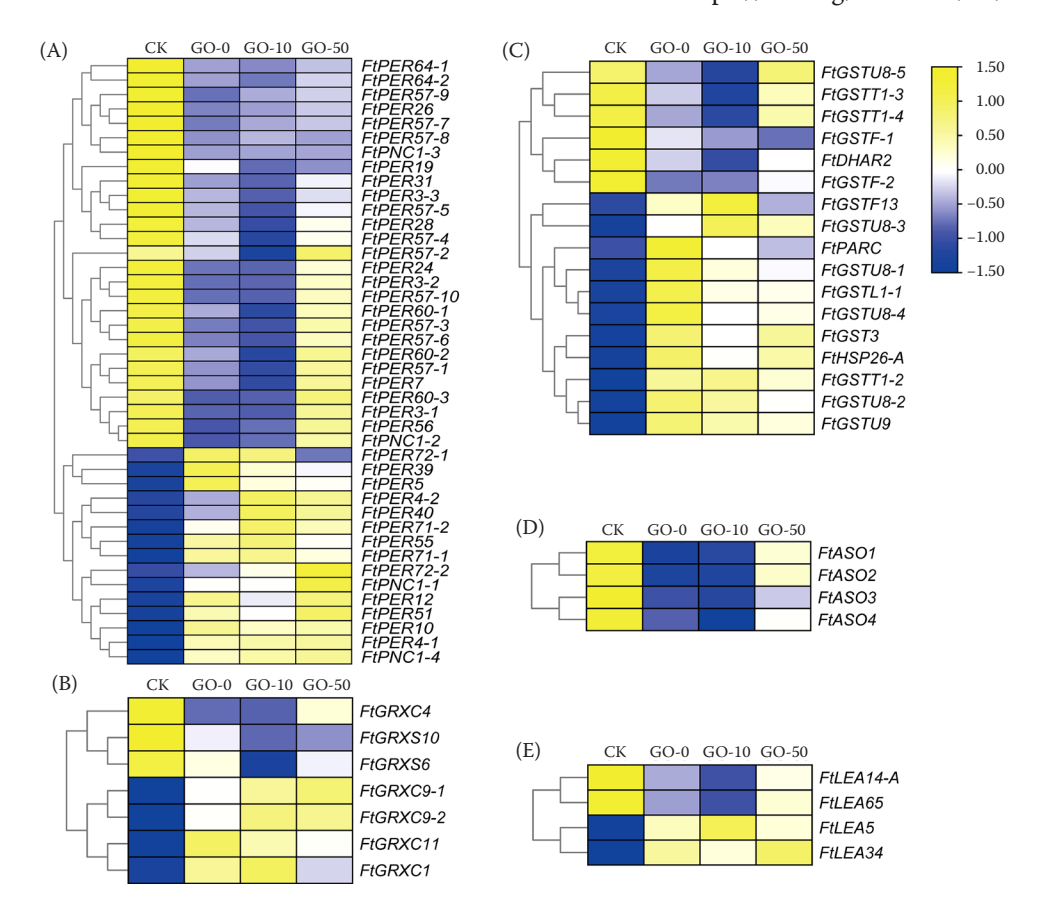


Figure 3. Expression analysis of genes involved in reactive oxygen species (ROS) detoxification under graphene oxide (GO) treatment: heatmap of peroxidase (*PER*) family genes (A), heatmap of glutaredoxin (*GRX*) family genes (B), heatmap of glutathione S-transferase (*GST*) family genes (C), heatmap of L-ascorbate oxidase (*ASO*) family genes (D), heatmap of late embryogenesis abundant protein (*LEA*) family genes (E)

Colour scale indicates the degree of expression; blue – low expression; yellow – high expression; CK represents the root treated with 0 mg/L GO. GO-0, GO-10 and GO-50 represent the GO with diameters of 0.5–3, 8–15 and > 50 μ m, respectively

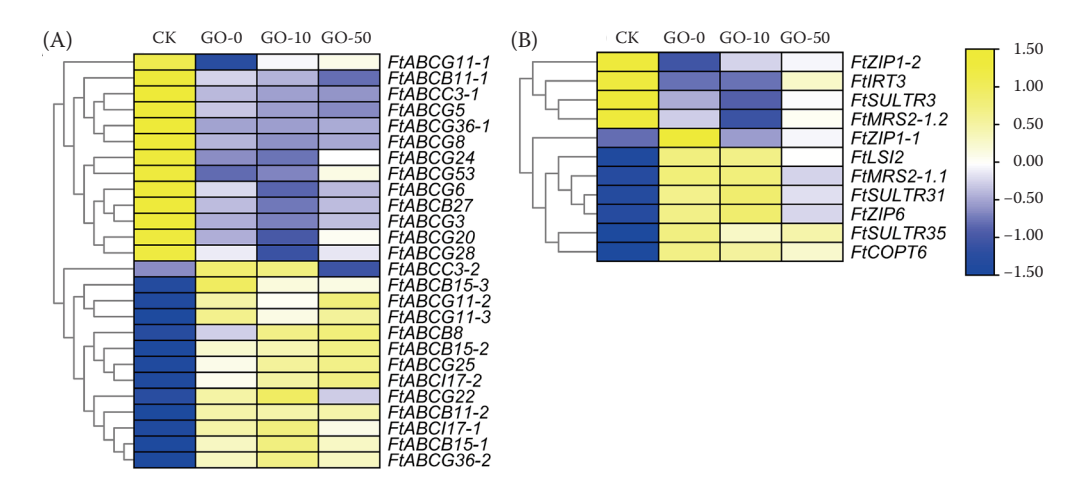


Figure 4. Expression analysis of genes encoding transporters under graphene oxide (GO) treatment: heatmap of ATP-binding cassette (ABC) transporter family genes (A), heatmap of other transporter encoding genes (B) Colour scale indicates the degree of expression; blue – low expression; yellow – high expression; CK represents the root treated with 0 mg/L GO; GO-0, GO-10 and GO-50 represent the GO with diameters of 0.5–3, 8–15 and > 50 μ m, respectively

down-regulated by GO, while the expression levels of other *ABC* genes were up-regulated (Figure 4A). Four genes, *FtZIP1-2*, *FtIRT3*, *FtSULTR3* and *FtMRS2-1.2*, showed lower expression levels under GO stress (Figure 4B). Besides, the expression of *FtSULTR31/35*, *FtZIP1-1/6*, *FtLSI2*, *FtMRS2-1.1* and *FtCOPT6* was up-regulated by GO.

Identification of DEGs encoding transcription factors (TFs). 84 DEGs encoding TF were identified, including 23 ethylene-responsive transcription fac-

tor (ERF), 14 WRKY, 11 basic leucine zipper (bZIP), eight GATA, eight homeobox-leucine zipper protein (HD-ZIP), eight heat stress TF (HSF), four MADS-box TF (MADS) and other TFs encoding genes (Table S5 in ESM). Of these *TFs*, most of *ERF*, *WRKY* and *HD-ZIP* genes' expression was up-regulated by GO stress, while most of *GATA* and *MADS* genes' expression was down-regulated (Figure 5). In addition, other *TF* genes are mainly showing two different expression patterns (Figure 5).

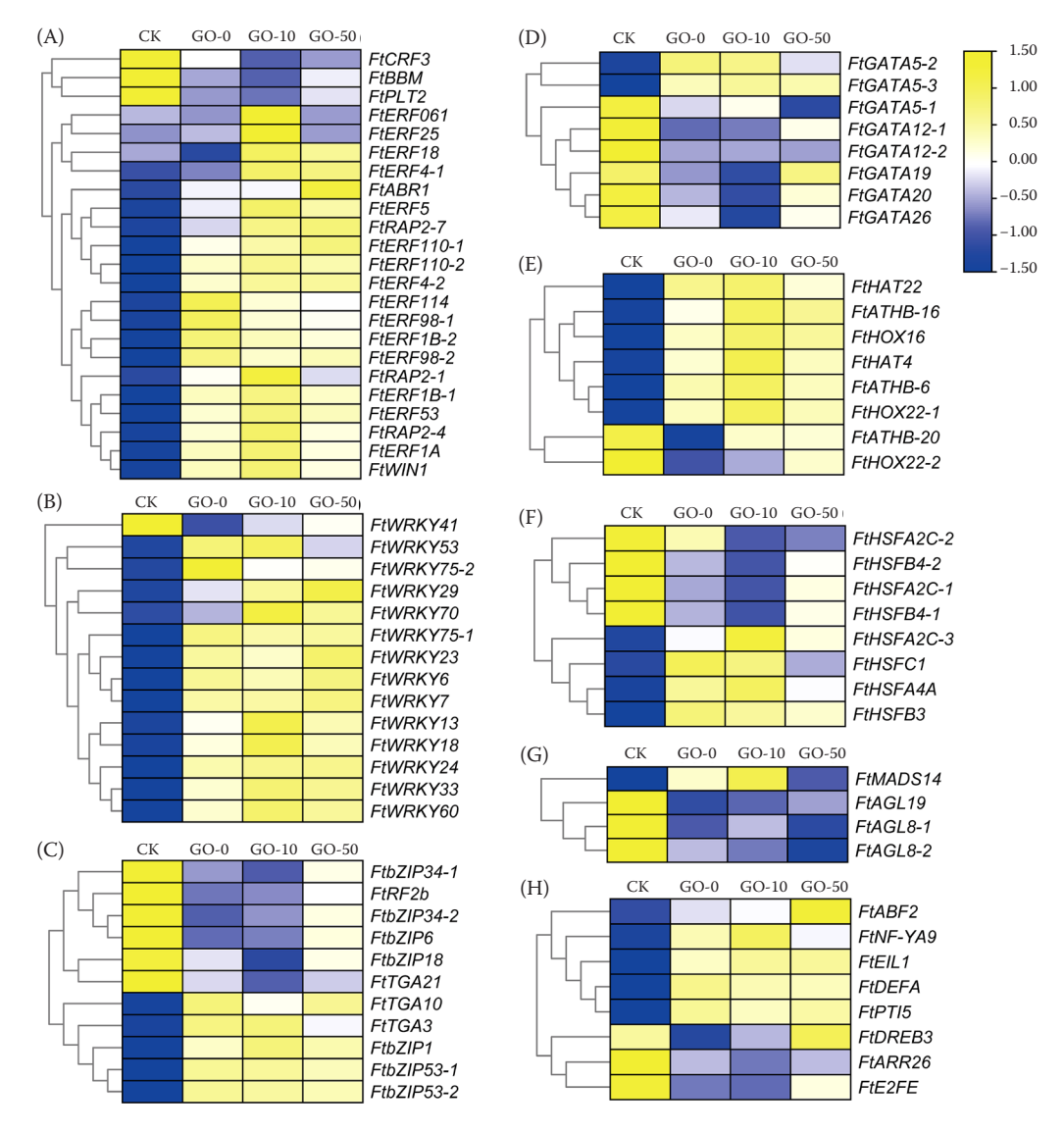


Figure 5. Expression analysis of genes encoding transcription factors (TFs) under graphene oxide (GO) treatment: heatmap of ethylene-responsive transcription factor (*ERF*) family genes (A), heatmap of *WRKY* family genes (B), heatmap of basic leucine zipper (*bZIP*) family genes (C), heatmap of *GATA* family genes (D), heatmap of homeobox-leucine zipper protein (*HD-ZIP*) family genes (E), heatmap of heat stress transcription factor (*HSF*) family genes (F), heatmap of *MADS* family genes (G), heatmap of other *TFs* (H)

Colour scale indicates the degree of expression; blue – low expression; yellow – high expression; CK represents the root treated with 0 mg/L GO; GO-0, GO-10 and GO-50 represent the GO with diameters of 0.5-3, 8-15 and >50 μ m, respectively

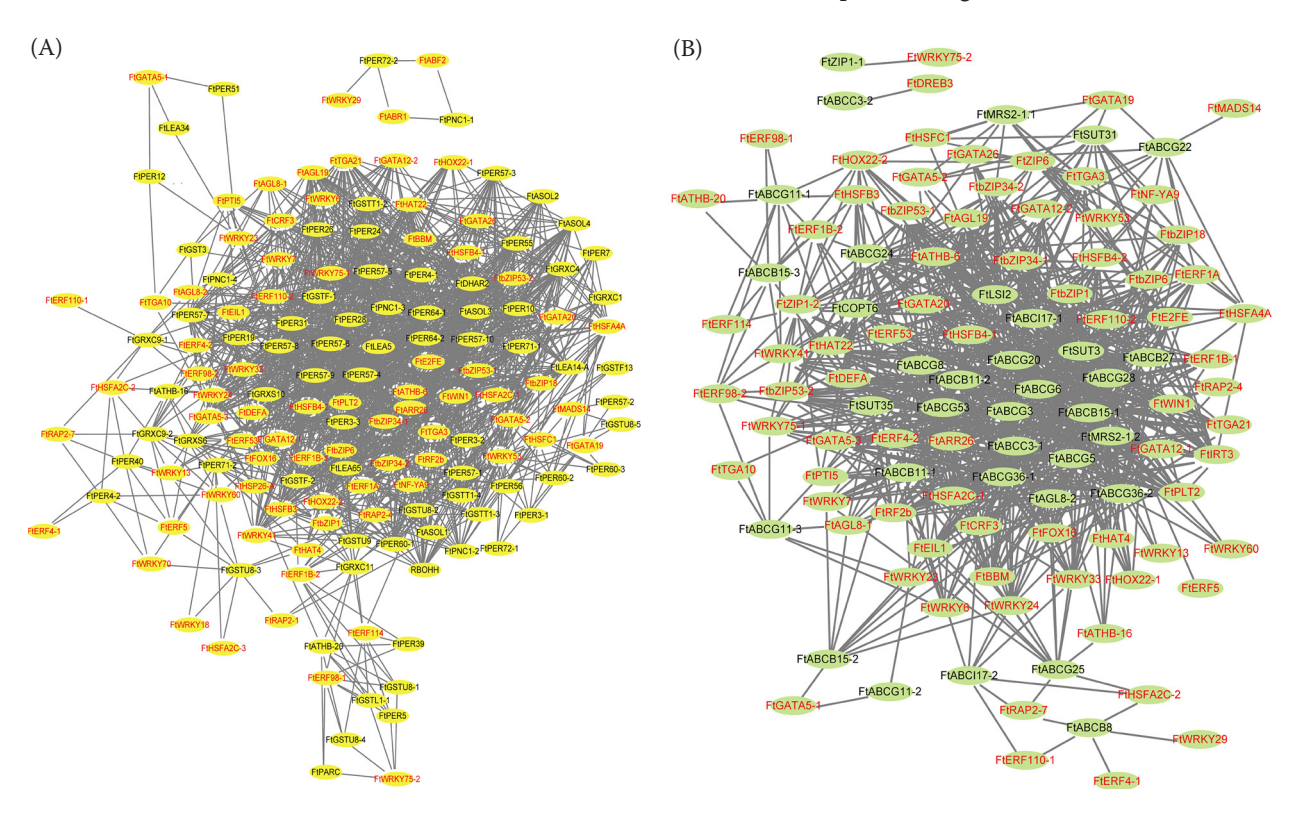


Figure 6. The correlations of reactive oxygen species (ROS) detoxification-related and transporter encoding genes with transcription factors (*TFs*) genes: the correlations between *TFs* and ROS detoxification-related genes (A), the correlations between *TFs* and transporter encoding genes (B)

The genes marked by red colour represent *TFs*; the genes marked by black represent ROS detoxification-related or transporter-encoding genes

Correlations between *TF* genes and transporters/ROS detoxification-related genes' expression were conducted. Most *TF* genes' expression had high correlations with that of transporters/ROS detoxification-related genes under GO stress (Figure 6). The above results provided insight into the transcriptional regulation of the GO-responsive transporters and ROS detoxification-related genes.

Identification of GO-responsive DEGs among the three GO materials with different diameters. The above data showed that GO-0, GO-10 and GO-50 distinctly influence root growth by biochemical and transcriptome analysis (Figure 1, 2), and the difference in the effect of these three GO materials on root was also investigated. 62 GO-diameter-dependent genes were generated (Figure 7A). Venn analysis showed that 49 of the 62 genes are GO-responsive DEGs (Figure 7B). Expression analysis showed that the 49 DEGs exhibited four expression patterns (Figure 7C). The expression of 20 genes, such as the genes encoding ABCC, CYP76AD1, GLP, GSTU, NAC21

and OPR2, was up-regulated by GO-0 and GO-10 but showed no response to GO-50. The expression levels of 18 genes, such as AUX22, EXO70A1, PER and XTH encoding genes, were down-regulated by GO-0 and GO-10 but showed no response to GO-50. The expression of ten genes, including DREB, GASA, GRXS and HHT encoding genes, was up-regulated by GO-50 but was down-regulated by GO-0 and GO-10. Additionally, 14 genes (such as ASR, CYP76B6, ERF, PP2C and YUC encoding genes) showed no response to GO-0 and their expression was up-regulated by GO-10 and GO-50 (Figure 7C).

DISCUSSION

The roots anchor the plant in the earth and perform close biological interactions with soil, and thus, roots are the first organ to encounter soil pollutants and hazardous materials (Zhao et al. 2023). With the wide application of GBMs, which have become the potential soil pollutants. Previous

studies revealed the toxic effects of GO on plant roots. GO with high concentrations significantly inhibited plant root growth (Cheng et al. 2016; Zhao et al. 2022b, 2023). High concentration of GO inhibited root growth by destroying the root cell structure, inducing oxidative stress and affecting normal root physiology (Jiao et al. 2016; Chen et al. 2018). In our previous study, GO can penetrate into buckwheat root and affect root growth (Liu et al. 2022). To improve our knowledge on the effects of GO on root growth, the response of buckwheat root to GO with different diameters was analysed. The results showed that all three GO materials negatively affect root growth (Figure 1), which in-

dicated the potential risk of GO in the agricultural production of buckwheat.

In previous studies, GO regulated root growth by modulating the expression of plant hormone biosynthesis and signalling genes (Li et al. 2018; Xie et al. 2019, 2020; Guo et al. 2021; Liu et al. 2022). However, there is no more information on the molecular mechanism of root response to GO. In this study, the molecular mechanism on the response to GO in buckwheat root was explored by transcriptome analysis. In total 3 724 GO-responsive DEGs were found in root (Figure 2). 70 DEGs involved in ROS detoxification and 37 potential transporters regulating GO transport were identified (Figure 3, 4).

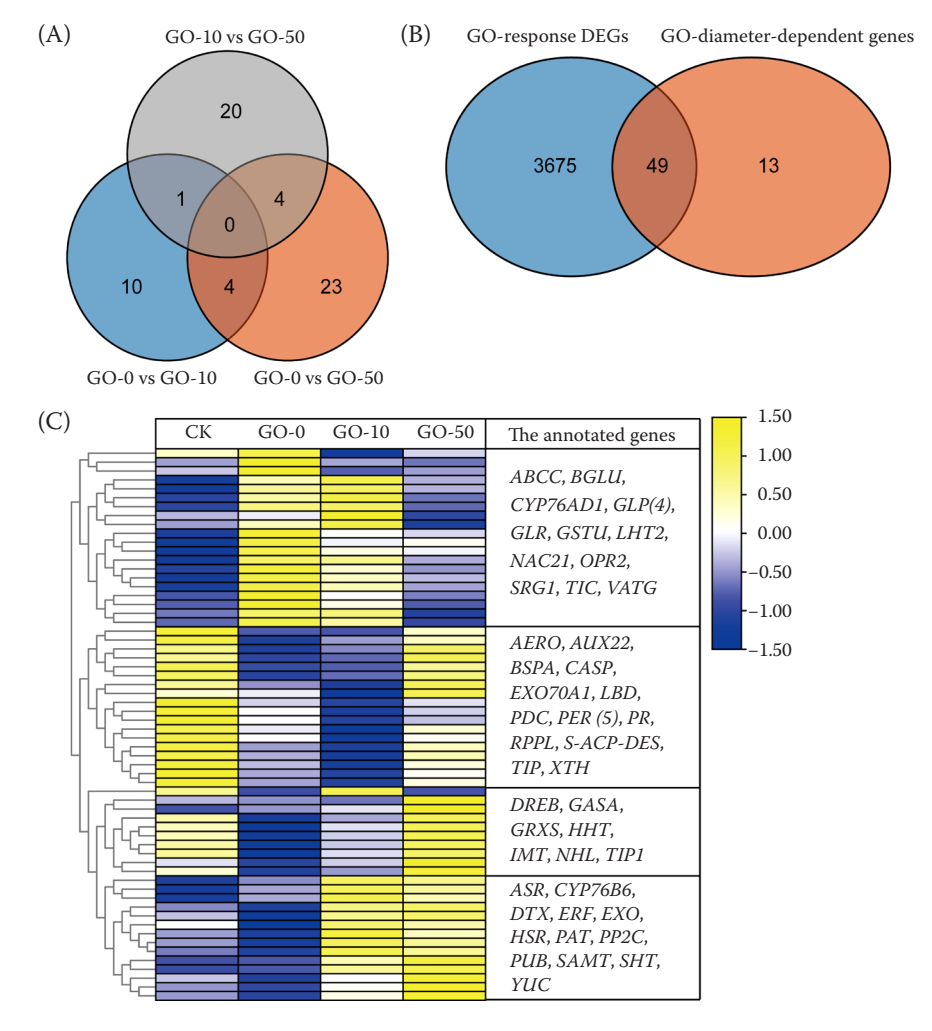


Figure 7. Identification of differentially expressed genes (DEGs) among the three graphene oxide (GO) materials with different diameters: Venn diagram showing the overlapping DEGs among the three GO materials (A), Venn diagram showing the GO-responsive genes among the three GO materials (B), heatmap of GO-responsive genes among the three GO materials, as well as identification of key DEGs (C)

Colour scale indicates the degree of expression; blue – low expression; yellow – high expression; CK represents the root treated with 0 mg/L GO; GO-0, GO-10 and GO-50 represent the GO with diameters of 0.5–3, 8–15 and > 50 μ m, respectively

In our previous study, the transporters involved in the uptake and transport of GO in buckwheat were also found (Liu et al. 2022). ABC transporters play a crucial role in various processes of plant growth and development, which are involved in toxic chemicals transport (Shen & Li 2023). The functions of these transporters are worthy of further study.

In this study, some genes from the 3 724 GOresponsive DEGs were found to be enriched into regulation of transcription DNA-templated (GO: 0006355) and DNA binding (GO: 0003677), which indicated TFs participating in the response of root to GO stress (Figure 2D). Here, 84 genes encoding TF were identified, including ERF, WRKY, bZIP, GATA, HD-ZIP, HSF, MADS and many other TFs (Table S5 in ESM). In B. napus, Pinus tabuliformis Carr. and maize (Zea mays L.), some TF genes were found to be involved in GO response (Cheng et al. 2016; Xie et al. 2019, 2020; Chen et al. 2021; Zhang et al. 2021a). Additionally, most of these TFs shared a high correlation with the expression of transporters and ROS detoxification-related genes under GO stress (Figure 6). The networks involved in the transcriptional regulation on the GO transport and ROS detoxification were suggested.

Some previous studies suggested GO with differences sizes showed distinct toxicity on plants. The layer numbers have a significant impact on the phytotoxicity of GO on Aloe vera L., buckwheat and wheat (Zhang et al. 2021b; Liu et al. 2022; Zhu et al. 2022). In this study, the toxicity of the GO with different diameter and similar layer on plants was first researched. It is found that higher diameters of GO may cause more adverse effects on root growth and stronger changes in ROS pathways (Figure 1), and the effect of GO on root growth may depend on its diameter. These genes, such as ABCC, CYP76AD1, GSTU, PER, NAC21, OPR2, AUX22, EXO70A1, XTH, DREB, ERF, PP2C and YUC encoding genes, were found to be involved in the difference on the toxicity of GO with different diameters (Figure 7). Additionally, it is unexpected that the number of GO-responsive DEGs under GO-50 is less than those under GO-0 and GO-10 (Figure 2A), which indicates that buckwheat root exhibited various responses to the GO with different diameters. However, much more works are needed to investigate the detailed molecular mechanism on the response of root to GO stress. This study improved our knowledge on GO response in plant root growth and provided new insight into the phytotoxic effects of GO with different sizes.

CONCLUSION

All three GO materials negatively affected root growth and induced ROS production. Higher diameters of GO caused more adverse effects on root. In total 3 724 GO-responsive DEGs were identified. Of these genes, 70 DEGs were involved in ROS detoxification and 37 transporter-encoding genes were found to be involved in GO response. These transporters may be involved in the uptake and transport of GO in buckwheat root. 84 TFs showed a response to GO stress in the root, which may regulate the transporters and ROS detoxification-related genes. Additionally, the difference on the transcriptomic response of root to different GO materials was investigated. 49 GO-responsive DEGs, such as ABCC, PER, NAC, DREB, ERF, PP2C and YUC encoding genes, may be involved in the difference on the toxicity of GO with different diameters. Our analysis provides new insights into the physiological and molecular mechanisms in relation to the phytotoxic effects of GO with various sizes.

REFERENCES

Alamdari S., Ghamsari M.S., Afarideh H., Mohammadi A., Geranmayeh S., Tafreshi M.J., Ehsani M.H., Majles ara M.H. (2019): Preparation and characterization of GO-ZnO nanocomposite for UV detection application. Optical Materials, 92: 243–250.

Basiuk V.A., Terrazas T., Luna-Martinez N., Basiuk E.V. (2019): Phytotoxicity of carbon nanotubes and nanodiamond in long-term assays with *Cactaceae* plant seedlings. Fullerenes Nanotubes and Carbon Nanostructures, 27: 141–149.

Chen J., Yang L., Li S., Ding W. (2018): Various physiological response to graphene oxide and amine-functionalized graphene oxide in wheat (*Triticum aestivum*). Molecules, 23: 1104

Chen Z., Zhao J., Song J., Han S., Du Y., Qiao Y., Liu Z., Qiao J., Li W., Li J., Wang H., Xing B., Pan Q. (2021): Influence of graphene on the multiple metabolic pathways of *Zea mays* roots based on transcriptome analysis. PLoS ONE, 16: e0244856.

Cheng F., Liu Y.F., Lu G.Y., Zhang X.K., Xie L.L., Yuan C.F., Xu B.B. (2016): Graphene oxide modulates root growth of *Brassica napus* L. and regulates ABA and IAA concentration. Journal of Plant Physiology, 193: 57–63.

Gao M., Xu Y., Chang X., Dong Y., Song Z. (2020): Effects of foliar application of graphene oxide on cadmium uptake by lettuce. Journal of Hazardous Materials, 98: 122859.

- Guo X., Zhao J., Wang R., Zhang H., Xing B., Naeem M., Yao T., Li R., Xu R., Zhang Z., Wu J. (2021): Effects of graphene oxide on tomato growth in different stages. Plant Physiology and Biochemistry, 162: 447–455.
- Hu C., Liu L., Li X., Xu Y., Ge Z., Zhao Y. (2018): Effect of graphene oxide on copper stress in *Lemna minor* L.: Evaluating growth, biochemical responses, and nutrient uptake. Journal of Hazardous Materials, 341: 168–176.
- Jiao J., Cheng F., Zhang X., Xie L., Li Z., Yuan C., Xu B., Zhang L. (2016): Preparation of graphene oxide and its mechanism in promoting tomato roots growth. Journal of Nanoscience and Nanotechnology, 16: 4216–4223.
- Lee J.Y., Kim M.J., Chung H. (2021): Effects of graphene oxide on germination and early growth of plants. Journal of Nanoscience and Nanotechnology, 21: 5282–5288.
- Li F., Sun C., Li X., Yu X., Luo C., Shen Y., Qu S. (2018): The effect of graphene oxide on adventitious root formation and growth in apple. Plant Physiology and Biochemistry, 129: 122–129.
- Liu C., Wu Q., Sun L., You X., Ye X., Wan Y., Wu X., Jiang L., Zhao G., Xiang D., Zou L. (2021): Nitrate dose-responsive transcriptome analysis identifies transcription factors and small secreted peptides involved in nitrogen response in Tartary buckwheat. Plant Physiology and Biochemistry, 162: 1–13.
- Liu C., Sun L., Sun Y., You X., Wan Y., Wu X., Tan M., Wu Q., Bai X., Ye X., Peng L., Zhao G., Xiang D., Zou L. (2022): Integrating transcriptome and physiological analyses to elucidate the molecular responses of buckwheat to graphene oxide. Journal of Hazardous Materials, 424: 127443.
- Liu S., Wei H., Li Z., Li S., Yan H., He Y., Tian Z. (2015): Effects of graphene on germination and seedling morphology in rice. Journal of Nanoscience and Nanotechnology, 15: 2695–2701.
- Luo Y., Wang X., Cao Y. (2021): Transcriptomic analysis suggested the involvement of impaired lipid droplet biogenesis in graphene oxide-induced cytotoxicity in human umbilical vein endothelial cells. Chemico-Biological Interactions, 333: 109325.
- Poulsen S.S., Bengtson S., Williams A., Jacobsen N.R., Troelsen J.T., Halappanavar S., Vogel U. (2021): A transcriptomic overview of lung and liver changes one day after pulmonary exposure to graphene and graphene oxide. Toxicology and Applied Pharmacology, 410: 115343.
- Shannon P., Markiel A., Ozier O., Baliga N.S., Wang J.T., Ramage D., Amin N., Schwikowski B., Ideker T. (2003): Cytoscape: A software environment for integrated models of biomolecular interaction networks. Genome Research, 13: 2498–2504.
- Shen C., Li X. (2023): Genome-wide identification and expression pattern profiling of the ATP-binding cassette

- gene family in tea plant (*Camellia sinensis*). Plant Physiology and Biochemistry, 202: 107930.
- Sun J., Zhou Q., Hu X. (2019): Integrating multi-omics and regular analyses identifies the molecular responses of zebrafish brains to graphene oxide: Perspectives in environmental criteria. Ecotoxicology and Environmental Safety, 180: 269–279.
- Tang M., Li J., He L., Guo R., Yan X., Li D., Zhang Y., Liao M., Shao B., Hu Y., Liu Y., Tang Q., Xia L., Guo X., Chai R. (2019): Transcriptomic profiling of neural stem cell differentiation on graphene substrates. Colloids and Surfaces B: Biointerfaces, 182: 110324.
- Weng Y., You Y., Lu Q., Zhong A., Liu S., Liu H., Du S. (2020): Graphene oxide exposure suppresses nitrate uptake by roots of wheat seedlings. Environmental Pollution, 262: 114224.
- Xie L.L., Chen F., Zou X.L., Shen S.S., Wang X.G., Yao G.X., Xu B.B. (2019): Graphene oxide and ABA cotreatment regulates root growth of *Brassica napus* L. by regulating IAA/ABA. Journal of Plant Physiology, 240: 153007.
- Xie L., Chen F., Du H., Zhang X., Wang X., Yao G., Xu B. (2020): Graphene oxide and indole-3-acetic acid cotreatment regulates the root growth of *Brassica napus* L. via multiple phytohormone pathways. BMC Plant Biology, 20: 101.
- Yang Y., Zhang R., Zhang X., Chen Z., Wang H., Li P.C.H. (2022): Effects of graphene oxide on plant growth: A review. Plants (Basel), 11: 2826.
- Zhang P., Zhang R., Fang X., Song T., Cai X., Liu H., Du S. (2016): Toxic effects of graphene on the growth and nutritional levels of wheat (*Triticum aestivum* L.): Shortand long-term exposure studies. Journal of Hazardous Materials, 317: 543–551.
- Zhang P., Guo Z., Luo W., Monikh F.A., Xie C., Valsami-Jones E., Lynch I., Zhang Z. (2020): Graphene oxideinduced pH alteration, iron overload, and subsequent oxidative damage in rice (*Oryza sativa* L.): A new mechanism of nanomaterial phytotoxicity. Environmental Science & Technology, 54: 3181–3190.
- Zhang X., Cao H., Wang H., Zhang R., Jia H., Huang J., Zhao J., Yao J. (2021a): Effects of graphene on morphology, microstructure and transcriptomic profiling of *Pinus tabuliformis* Carr. roots. PLoS ONE, 16: e0253812.
- Zhang X., Cao H., Zhao J., Wang H., Xing B., Chen Z., Li X., Zhang J. (2021b): Graphene oxide exhibited positive effects on the growth of *Aloe vera* L. Physiology and Molecular Biology of Plants, 27: 815–824.
- Zhang X., Cao H., Wang H., Zhao J., Gao K., Qiao J., Li J., Ge S. (2022): The effects of graphene-family nanomaterials on plant growth: A review. Nanomaterials (Basel), 12: 936.

- Zhang Y., Tian X., Huang P., Yu X., Xiang Q., Zhang L., Gao X., Chen Q., Gu Y. (2023): Biochemical and transcriptomic responses of buckwheat to polyethylene microplastics. Science of the Total Environment, 899: 165587.
- Zhao L., Wang W., Fu X., Liu A., Cao J., Liu J. (2022a): Graphene oxide, a novel nanomaterial as soil water retention agent, dramatically enhances drought stress tolerance in soybean plants. Frontiers in Plant Science, 13: 810905.
- Zhao S., Wang Q., Zhao Y., Rui Q., Wang D. (2015): Toxicity and translocation of graphene oxide in *Arabidopsis thaliana*. Environmental Toxicology and Pharmacology, 39: 145–156.
- Zhao S., Zhu X., Mou M., Wang Z., Duo L. (2022b): Assessment of graphene oxide toxicity on the growth and nutrient levels of white clover (*Trifolium repens* L.). Ecotoxicology and Environmental Safety, 234: 113399.

- Zhao S., Wang W., Chen X., Gao Y., Wu X., Ding M., Duo L. (2023): Graphene oxide affected root growth, anatomy, and nutrient uptake in alfalfa. Ecotoxicology and Environmental Safety, 250: 114483.
- Zhu Y.X., Weng Y.N., Zhang S.Y., Liu L.J., Du S.T. (2022): The nitrate uptake and growth of wheat were more inhibited under single-layer graphene oxide stress compared to multi-layer graphene oxide. Ecotoxicology and Environmental Safety, 247: 114229.

Received: June 18, 2024 Accepted: July 30, 2024 Published online: August 22, 2024